J. Min. Metall. Sect. B-Metall. 51 (2) B (2015) 125 - 132

Journal of Mining and Metallurgy, Section B: Metallurgy

THERMODYNAMIC REASSESSMENT OF THE Mn-Ni-Si SYSTEM

B. Hu[a,b,*], Y. Du[b], J.-J. Yuan[a], Z.-F. Liu[a], Q.-P. Wang[a]

[a] School of Materials Science and Engineering, Anhui University of Science and Technology, Huainan, China
[b] State Key Laboratory of Powder Metallurgy, Central South University, Changsha, Hunan, China

(Received 02 October 2014; accepted 28 April 2015)

Abstract

Based on the new experimental data available in the literature, the Mn-Ni-Si system has been reassessed using the CALPHAD (CALculation of PHAse Diagram) approach. Compared with the previous modeling, the τ_8 and τ_{12} ternary phases were treated as the same phase according to the new experimental data. The Mn_3Si phase was described with two sublattice model $(Mn, Ni)_3(Si)_1$. The reported new ternary phase τ was not considered in the present work. Comprehensive comparisons between the calculated and measured phase diagrams showed that a set of thermodynamic parameters of the Mn-Ni-Si system obtained in this work was more accurate than the previous one.

Keywords: Mn-Ni-Si system; CALPHAD; Phase diagram; Thermodynamic calculation

1. Introduction

The Mn-Ni-Si ternary system is of great interest because it is one of technically important systems containing the G ($Mn_6Ni_{16}Si_7$) phase [1]. In addition to the technological importance, the Mn-Ni-Si system is an important ternary system in Al-based alloys. As one of the common alloying elements, Mn plays an important role in preventing recrystallization and grain growth, and hence refining grains. Ni and Si are also ones of the major alloying elements in Al alloys. In our effort to develop a thermodynamic database for multi-component Al-alloys [2-6], it is realized that a more accurate thermodynamic description of the Mn-Ni-Si system is needed along with three constitutive binary systems.

A thermodynamic modeling of the Mn-Ni-Si system has been reported by our previous work [1] based on the reliable experimental data available in the literature supplemented with our own experiments and first-principles calculations. The previous thermodynamic description can satisfactorily account for most of the contemporaneous available experimental data. However, the thermodynamic parameters cannot well reproduce the new reported experimental data [7]. Hence, it is necessary to reassess the Mn-Ni-Si system in order to obtain a set of more accurate thermodynamic parameters.

The purposes of the present work are to critically evaluate the new reported experimental data and to obtain an optimal set of thermodynamic parameters for the Mn-Ni-Si system over the entire composition range.

2. Evaluation of experimental data in the literature

Since the previous experimental phase equilibria data of the Mn-Ni-Si system have been reviewed in our work [1], they are briefly presented here and the new reported experimental data are evaluated in detail. The Mn-Ni-Si system has been experimentally investigated by Cherkashin et al. [8], Kuz'ma [9], Kuz'ma and Cherkashin [10], Kuz'ma et al. [11] and Bardos et al. [12]. Two ternary phases, i.e. the τ_4 phase with the composition close to MnNiSi and the τ_5 phase with a variable composition around $Mn_3Ni_3Si_2$, were firstly reported by Cherkashin et al. [8]. A partial isothermal section at the Mn corner at 800 °C was proposed by Kuz'ma [9]. Subsequently, the same group of authors [11] presented a complete 800 °C isothermal section based on the examination of 240 alloys. Ten ternary compounds (τ_1 to τ_{10}) were found at 800 °C. A partial isothermal section at the Mn-rich corner at 1000 °C was published by Bardos et al. [12]. According to Bardos et al. [12], the previously reported τ_8 phase [11] was not found at 1000 °C while a new phase τ_{12} was detected within the same composition region. Between τ_7 and τ_{12}, another phase τ_{11} was found at the composition of $Mn_{52}Ni_{29}Si_{19}$. In addition, the τ_9 and τ_{10} phases were not detected at 1000 °C. The Mn-Ni-Si ternary system was reviewed by Gupta [13], who considered the previous experimental results [9-12].

Recently, 52 ternary alloys were prepared and annealed at 900 °C for 30 days and the isothermal

* *Corresponding author: bhu@aust.edu.cn*

DOI:10.2298/JMMB141002015H

section at 900 °C over the entire composition range in the Mn-Ni-Si system was established by Liang [7] using X-ray diffraction and scanning electron microscope. The experimental results were presented as follows in detail. Seven ternary compounds (τ_1 to τ_7) were confirmed and τ_9 and τ_{10} were not found at 900 °C, which were consistent with the isothermal sections at 800 and 1000 °C measured by Kuz'ma et al. [11], Hu et al. [1] and Bardos et al. [12], respectively. A new ternary compound τ was discovered with the composition at about $Mn_{45}Ni_{40}Si_{15}$, which experienced martensitic phase transformation during the quenching. The crystal structure of the martensitic phase was determined to be hexagonal structure with cell parameters of *a* = 0.47783(8) *nm* and *c* = 0.76847(9) *nm*. The crystal structure of τ_1 was firstly identified to be hexagonal structure with cell parameters of *a* = 1.70738(8) *nm* and *c* = 0.7841(9) *nm*. Moreover, the structure type and the space group of this compound were determined to be Co_4NbSi_3 and No.191, respectively. The reported τ_8 and τ_{12} ternary phases were identified to be the same compound and to be isostructural to $V_{41}Ni_{36}Si_{23}$ with monoclinic structure. The cell parameters were roughly calculated to be *a* = 1.359 *nm*, *b* = 2.358 *nm*, β=100.1° and *c* = 0.901 *nm*. In addition, the solubility of Ni in the Mn_3Si phase was about 5.5 at.% Ni.

3. Thermodynamic modeling

In the present modeling, the Gibbs energy functions for the elements Mn, Ni and Si are taken from the SGTE database compiled by Dinsdale [14]. The thermodynamic parameters for the Mn-Ni, Mn-Si, and Ni-Si systems are taken from Liu [15], Du et al. [16] and Schuster and Du [17], respectively.

The solution phases, i.e. liquid and Cub_A13, are described by the substitutional solution model. The excess Gibbs energy of the solution phases is described by the Redlich-Kister-Muggianu polynomial [18]. The binary and ternary interaction parameters can be expressed as L = A + B * T, and the coefficients *A* and *B* are evaluated from experimental data.

The binary phases MnSi, Mn_5Si_3, Mn_3Si and $NiSi_2$, which were experimentally observed to considerably extend into the ternary system with Ni and Mn atoms substituting for each other, are described with the sublattice models $(Mn, Ni)_1Si_1$, $(Mn, Ni)_5Si_3$, $(Mn, Ni)_3Si_1$ and $(Ni, Mn)_1Si_2$, respectively. The bold fonts indicate the major atoms in the sublattices.

The ordered $L1_2$ and Bcc_B2 phases are modeled as $(Mn, Ni, Si)_{0.75}(Mn, Ni, Si)_{0.25}Va_1$ and $(Mn, Ni, Si, Va)_{0.5}(Mn, Ni, Si, Va)_{0.5}Va_3$, respectively. In order to use a single function to describe the Gibbs energies of both the ordered and disordered phases, the disordered Fcc_A1 and Bcc_A2 are described with $(Mn, Ni, Si)_1Va_1$ and $(Mn, Ni, Si, Va)_1Va_1$, respectively.

In view of experimentally observed negligible homogeneity range and unknown crystal structure information [7-10], the ternary compounds, τ_1-τ_4, τ_7 and τ_9-τ_{11}, are treated as stoichiometric ones. Taking into account crystal structures and experimental homogeneities [5, 9], the two Laves phases τ_5 and τ_6 are described with the sublattice model $Mn_1(Ni,Si)_2$ and the τ_8 and τ_{12} phases are treated as the same phase with the sublattice model $(Mn,Ni)_3Si_1$. The detailed description of the thermodynamic modeling can be found in our previous work [1].

4. Results and discussion

The thermodynamic parameters were evaluated by the optimization module PARROT [19] of the program Thermo-Calc, which works by minimizing the square sum of the differences between measured and calculated values. The step-by-step optimization procedure carefully described by Du et al. [20] was utilized in the present assessment.

The optimization is based on our previous work [1]. By using the reliable experimental data [1, 7, 11, 12] selected from the literature, the model parameters for solution phases (liquid and Cub_A13), ordered/disordered phases ($L1_2$/Fcc_A1 and Bcc_B2/Bcc_A2), binary phases extending into the ternary system (MnSi, Mn_5Si_3, Mn_3Si and $NiSi_2$) and eleven ternary phases (τ_1 to τ_{11}) could be optimized. The thermodynamic parameters finally obtained in the present work are listed in Table 1.

The calculated isothermal sections at 800, 900 and 1000 °C of the Mn-Ni-Si system along with the experimental data from the literature [1, 7, 11, 12] are shown in Figures 1-3, respectively. The calculated isothermal sections can reproduce most of the experimental data reasonably. The calculated solubility of Ni in the Mn_3Si phase 6.5 at.% Ni is consistent with experimental data [7]. As can be seen from Figure 2, the new ternary compound τ reported by Liang [7] is not considered on the basis of the following two aspects. On the one hand, according to the work of Liang [7], only γMnNi (Fcc_A1) and βMn (Cub_A13) are included in the Mn-Ni system at 900 °C and the body-centered tetragonal structure MnNi (Bcc_B2) is not found when equilibrium is reached. This result is inconsistent with the generally accepted Mn-Ni phase diagram (see Figure 1(a) in [1]). More experiments are needed to confirm this point. On the other hand, in view of the large solubility of Si in the Bcc_B2 phase at 800 °C in Figure 1 and the composition of the new ternary compound τ closing to the Bcc_B2, the τ phase is likely to be a solid solution of Bcc_B2 in the Mn-Ni-Si system. Hence, the τ phase is not included in the present optimization.

Table 1. *Summary of the reassessed thermodynamic parameters in the Mn-Ni-Si system*[a]

Phase/model	Thermodynamic parameters	Reference
Liuqid: $(Mn, Ni, Si)_1$	${}^{1}L^{Liquid}_{Mn,Ni,Si} = -120000$	This work
	${}^{2}L^{Liquid}_{Mn,Ni,Si} = -55000$	This work
[b]Fcc_A1: $(Mn, Ni, Si)_1(Va)_1$	${}^{o}L^{Fcc\_A1}_{Mn,Ni,Si:Va} = -279173.878$	[1]
	${}^{1}L^{Fcc\_A1}_{Mn,Ni,Si:Va} = +5888.419$	[1]
[b]$L1_2$: $(Mn, Ni, Si)_{0.75}(Mn, Ni, Si)_{0.25}(Va)_1$	${}^{o}L^{L1_2}_{Mn,Ni:Si:Va} = -55959.365 - 9.842 \cdot T$	[1]
	${}^{o}L^{L1_2}_{Mn,Si:Ni:Va} = -609.633$	[1]
	${}^{o}L^{L1_2}_{Ni,Si:Mn:Va} = -104576.464 - 0.230 \cdot T$	[1]
	${}^{1}L^{L1_2}_{Mn,Ni:Si:Va} = 14985.355 + 9.842 \cdot T$	[1]
	${}^{1}L^{L1_2}_{Mn,Si:Ni:Va} = -203.211$	[1]
	${}^{1}L^{L1_2}_{Ni,Si:Mn:Va} = -14720.6612 - 9.842 \cdot T$	[1]
	${}^{o}L^{L1_2}_{Mn,Ni,Si:Mn:Va} = 18107.344 + 9.842 \cdot T$	[1]
	${}^{o}L^{L1_2}_{Mn,Ni,Si:Ni:Va} = -54479.906 - 39.367 \cdot T$	[1]
	${}^{o}L^{L1_2}_{Mn,Ni,Si:Si:Va} = 14985.355 + 9.842 \cdot T$	[1]
	${}^{o}L^{L1_2}_{Mn,Ni:Ni,Si:Va} = -5121.751$	[1]
	${}^{o}L^{L1_2}_{Ni,Si:Mn,Ni:Va} = -5121.751$	[1]
	${}^{o}L^{L1_2}_{Mn,Ni:Mn,Si:Va} = -5121.751$	[1]
	${}^{o}L^{L1_2}_{Mn,Si:Mn,Ni:Va} = -5121.751$	[1]
	${}^{o}L^{L1_2}_{Mn,Si:Ni,Si:Va} = -2560.876$	[1]
	${}^{o}L^{L1_2}_{Ni,Si:Mn,Si:Va} = -2560.876$	[1]
[c]Bcc_A2: $(Mn, Ni, Si, Va)_1(Va)_3$	${}^{o}L^{Bcc\_A2}_{Mn,Ni,Si:Va} = -360523.246$	[1]
	${}^{1}L^{Bcc\_A2}_{Mn,Ni,Si:Va} = -417536.599$	[1]
[c]Bcc_B2: $(Mn,Ni,Si,Va)_{0.5}(Mn,Ni,Si,Va)_{0.5}(Va)_3$	${}^{o}L^{Bcc\_B2}_{Mn,Si:Ni:Va} = -182448.464 + 110 \cdot T$	[1]
	${}^{o}L^{Bcc\_B2}_{Ni:Mn,Si:Va} = -182448.464 + 110 \cdot T$	[1]
	${}^{o}L^{Bcc\_B2}_{Ni,Si:Mn:Va} = -45888.881$	[1]
	${}^{o}L^{Bcc\_B2}_{Mn:Ni,Si:Va} = -45888.881$	[1]
Cub_A13: $(Mn, Ni, Si)_1(Va)_1$	${}^{o}L^{Cub}_{Mn,Ni,Si:Va} = -949446.509 + 300 \cdot T$	This work
	${}^{2}L^{Cub}_{Mn,Ni,Si:Va} = -701707.49 + 300 \cdot T$	This work
MnSi: $(Mn, Ni)_{1/2}(Si)_{1/2}$	${}^{o}G^{MNSi}_{Ni:Si} = -37250 + 1/2\ {}^{o}G^{Fcc}_{Ni} + 1/2\ {}^{o}G^{Dia}_{Si}$	[1]
	${}^{o}L^{MnSi}_{Mn,Ni:Si} = -11655.852 + 7.134 \cdot T$	[1]
	${}^{1}L^{MnSi}_{Mn,Ni:Si} = 30454.435 - 20 \cdot T$	[1]
Mn_5Si_3: $(Mn, Ni)_{5/8}(Si)_{3/8}$	${}^{o}G^{Mn_5Si_3}_{Ni:Si} = -42000 + 2.75 \cdot T + 5/8\ {}^{o}G^{Fcc}_{Ni} + 3/8\ {}^{o}G^{Dia}_{Si}$	[1]
	${}^{o}L^{Mn_5Si_3}_{Mn,Ni:Si} = -20428.317 + 8.604 \cdot T$	[1]
	${}^{1}L^{Mn_5Si_3}_{Mn,Ni:Si} = -28361.277 + 3.133 \cdot T$	[1]

Table continued on the next page

Table continued from the previous page

Mn_3Si: $(Mn, Ni)_{3/4}(Si)_{1/4}$	${}^oG_{Ni:Si}^{Mn_3Si} = -19634.25 - 5\cdot T + 3/4\ {}^oG_{Ni}^{Fcc} + 1/4\ {}^oG_{Si}^{Dia}$ ${}^oL_{Mn,Ni:Si}^{Mn_3Si} = -45000$	This work This work
$NiSi_2$: $(Ni, Mn)_{1/3}(Si)_{2/3}$	${}^oG_{Mn:Si}^{NiSi_2} = -11334.545 + 1/3\ {}^oG_{Mn}^{Cbcc} + 2/3\ {}^oG_{Si}^{Dia}$ ${}^oL_{Ni,Mn:Si}^{NiSi_2} = -12131.638$	[1] [1]
τ_1: $Mn_{0.15}Ni_{0.45}Si_{0.40}$	${}^oG_{Mn:Ni:Si}^{\tau_1} = -23722.932 - 18\cdot T + 0.15\ {}^oG_{Mn}^{Cbcc} + 0.45\ {}^oG_{Ni}^{Fcc} + 0.40\ {}^oG_{Si}^{Dia}$	[1]
τ_2: $Mn_{0.15}Ni_{0.50}Si_{0.35}$	${}^oG_{Mn:Ni:Si}^{\tau_2} = -34731.0497 - 9.3\cdot T + 0.15\ {}^oG_{Mn}^{Cbcc} + 0.50\ {}^oG_{Ni}^{Fcc} + 0.35\ {}^oG_{Si}^{Dia}$	This work
τ_3: $Mn_{6/29}Ni_{16/29}Si_{7/29}$	${}^oG_{Mn:Ni:Si}^{\tau_3} = -54625.3969 + 6\cdot T + 6/29\ {}^oG_{Mn}^{Cbcc} + 16/29\ {}^oG_{Ni}^{Fcc} + 7/29\ {}^oG_{Si}^{Dia}$	This work
τ_4: $Mn_{1/3}Ni_{1/3}Si_{1/3}$	${}^oG_{Mn:Ni:Si}^{\tau_4} = -28381.4464 - 15.5\cdot T + 1/3\ {}^oG_{Mn}^{Cbcc} + 1/3\ {}^oG_{Ni}^{Fcc} + 1/3\ {}^oG_{Si}^{Dia}$	This work
τ_5: $Mn_{1/3}(Ni,Si)_{2/3}$	${}^oG_{Mn:Ni}^{\tau_5} = -6718.0582 - T + 1/3\ {}^oG_{Mn}^{Cbcc} + 2/3\ {}^oG_{Ni}^{Fcc}$ ${}^oG_{Mn:Si}^{\tau_5} = 20981.9005 - 4\cdot T + 1/3\ {}^oG_{Mn}^{Cbcc} + 2/3\ {}^oG_{Si}^{Dia}$ ${}^oL_{Mn:Ni,Si}^{\tau_5} = -180909.102$ ${}^1L_{Mn:Ni,Si}^{\tau_5} = -13500$	This work This work [1] [1]
τ_6: $Mn_{1/3}(Ni,Si)_{2/3}$	${}^oG_{Mn:Ni}^{\tau_6} = 9013.8439 + T + 1/3{}^oG_{Mn}^{Cbcc} + 2/3{}^oG_{Ni}^{Fcc}$ ${}^oG_{Mn:Si}^{\tau_6} = 1666.667 + 1/3\ {}^oG_{Mn}^{Cbcc} + 2/3\ {}^oG_{Si}^{Dia}$ ${}^oL_{Mn:Ni,Si}^{\tau_6} = -159474.806$ ${}^1L_{Mn:Ni,Si}^{\tau_6} = -172110.472$	This work [1] [1] [1]
τ_7: $Mn_{3/6}Ni_{2/6}Si_{1/6}$	${}^oG_{Mn:Ni:Si}^{\tau_7} = -27712.39 - 9.4\cdot T + 3/6\ {}^oG_{Mn}^{Cbcc} + 2/6\ {}^oG_{Ni}^{Fcc} + 1/6\ {}^oG_{Si}^{Dia}$	This work
τ_8/τ_{12}: $(Mn,Ni)_{3/4}Si_{1/4}$	${}^oG_{Mn:Si}^{\tau_8} = -4502.813 + 3/4\ {}^oG_{Mn}^{Cbcc} + 1/4\ {}^oG_{Si}^{Dia}$ ${}^oG_{Ni:Si}^{\tau_8} = -7503.769 + 3/4\ {}^oG_{Ni}^{Fcc} + 1/4\ {}^oG_{Si}^{Dia}$ ${}^oL_{Mn,N:Si}^{\tau_8} = -112966.849$ ${}^1L_{Mn,Ni:Si}^{\tau_8} = -74906.402$	[1] [1] [1] [1]
τ_9: $Mn_{0.61}Ni_{0.12}Si_{0.27}$	${}^oG_{Mn:Ni:Si}^{\tau_9} = -44973.9426 + 10\cdot T + 0.61{}^oG_{Mn}^{Cbcc} + 0.12{}^oG_{Ni}^{Fcc} + 0.27{}^oG_{Si}^{Dia}$	This work
τ_{10}: $Mn_{0.66}Ni_{0.04}Si_{0.30}$	${}^oG_{Mn:Ni:Si}^{\tau_{10}} = -34946.208 + 5\cdot T + 0.66{}^oG_{Mn}^{Cbcc} + 0.04{}^oG_{Ni}^{Fcc} + 0.30{}^oG_{Si}^{Dia}$	This work
τ_{11}: $Mn_{0.52}Ni_{0.29}Si_{0.19}$	${}^oG_{Mn:Ni:Si}^{\tau_{11}} = -17541.82 - 17.2\cdot T + 0.52{}^oG_{Mn}^{Cbcc} + 0.29{}^oG_{Ni}^{Fcc} + 0.19{}^oG_{Si}^{Dia}$	This work

[a]All parameters are given in J/(mole of atoms); Temperature (T) in K.
[b]The ordered phase $L1_2$ and disordered phase Fcc_A1 are modeled as the same phase.
[c]The ordered phase Bcc_B2 and disordered phase Bcc_A2 are modeled as the same phase.

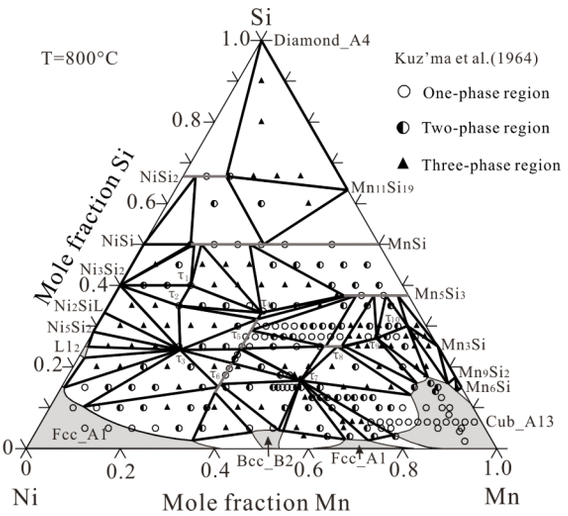

Figure 1. *Calculated isothermal section at 800 °C of the Mn-Ni-Si system along with the experimental data from Kuz'ma et al. [11].*

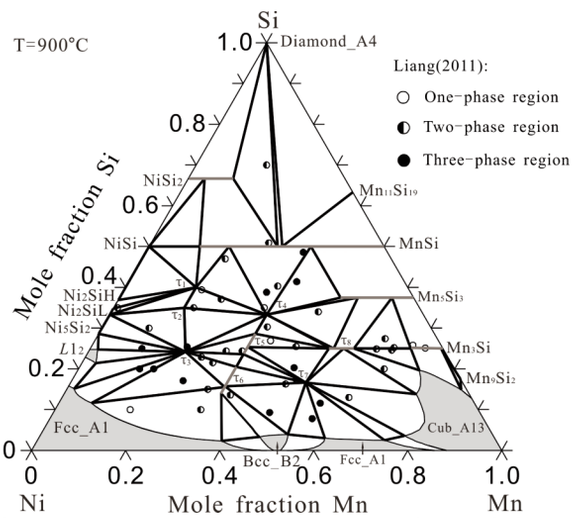

Figure 2. *Calculated isothermal section at 900 °C of the Mn-Ni-Si system along with the experimental data from Liang [7].*

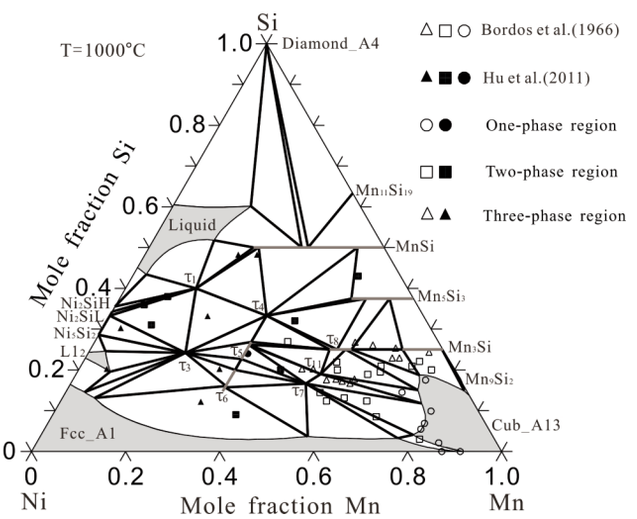

Figure 3. *Calculated isothermal section at 1000 °C of the Mn-Ni-Si system along with the experimental data from Hu et al. [1] and Bordos et al. [12].*

In addition, it is noteworthy that there is a sharp edge on the τ_6 in the two-phase region τ_6 + Fcc_A1 at 1000 ºC in Figure 3. The present calculated results are reasonable in view of the following two reasons. First, the shape of τ_6 is determined by both thermodynamic parameters of the τ_6 phase and those of other phases around τ_6, which are globally optimized based on the phase-equilibrium and thermodynamic properties. Second, a sharp edge on the τ_6 in the two-phase region τ_6 + Fcc_A1 is expected to exist at a temperature above 900ºC. This can be deduced from the difference between the phase relations at 1000 and 900ºC of the Mn-Ni-Si system. There exist the three-phase regions of τ_6 + Fcc_A1 + Bcc_B2, τ_6 + τ_3 + Fcc_A1 and τ_7 + τ_6 + Bcc_B2 at 900 ºC in Figure 2, and the compositions of τ_6 for the 3 three-phase regions are not identical. However, there exist τ_3 + τ_6 + Fcc_A1 and τ_6 + τ_7 + Fcc_A1 three-phase regions at 1000 ºC in Figure 3. Based on the phase rule, there should be a sharp edge on the τ_6 in the two-phase region τ_6 + Fcc_A1 at the temperatures above 900 ºC, which will disappear at higher temperatures. This exact temperature should be measured in the future experiments, but is not the purpose of the present work.

The calculated liquidus projection and reaction scheme of the Mn-Ni-Si system according to the present thermodynamic parameters are presented in Figures 4 and 5, respectively. The liquidus projection and reaction scheme have been proved to be a useful tool in describing ternary and higher component systems.

5. Conclusions

The new reported experimental phase diagram data for the Mn-Ni-Si system was critically evaluated. The Mn-Ni-Si system has been reassessed using the CALPHAD approach over entire composition range taking into account the experimental data from the literature, and an optimal set of thermodynamic parameters of the Mn-Ni-Si system was obtained. The calculated results agreed well with the experimental data.

Acknowledgments

The financial support from the National Basic Research Program of China (No. 2014CB644002), the National Natural Science Foundation of China (No. 51501002), the Scientific Research Starting Foundation for the Introduced Talents of Anhui University of Science and Technology Project (No. ZX979), and Thermo-Calc Software AB under the Aluminum Alloy Database Project are greatly acknowledged.

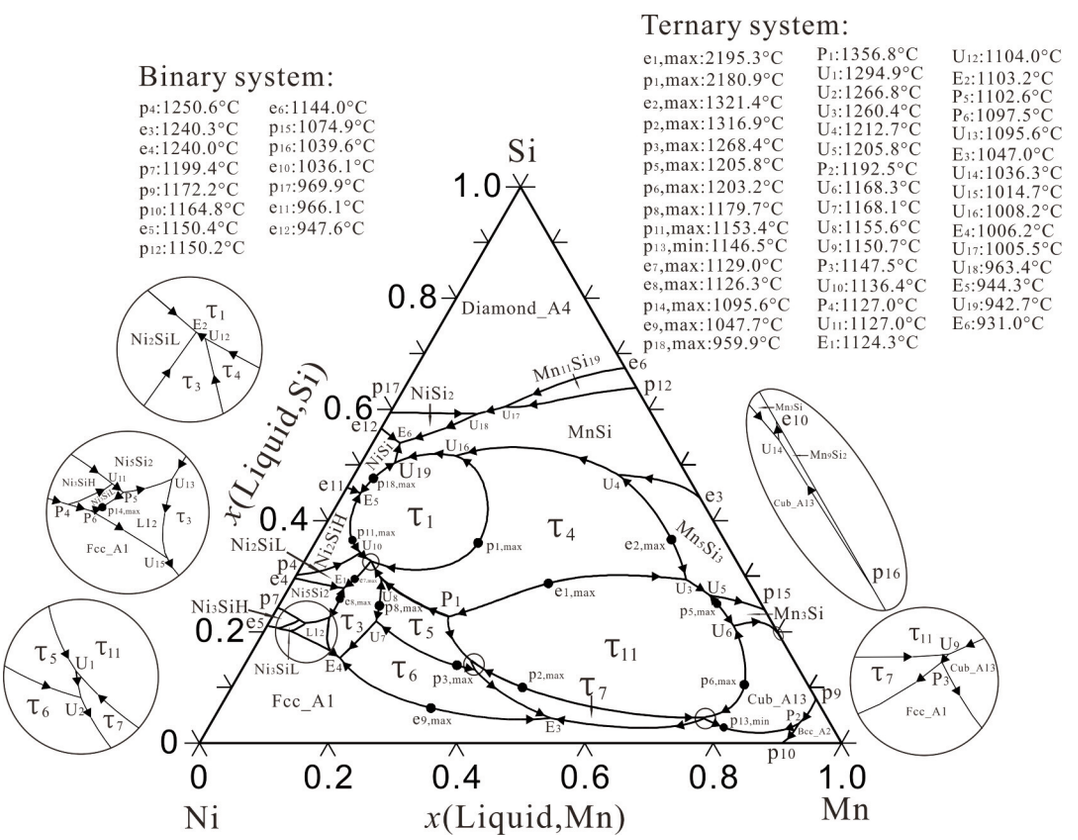

Figure 4. *Calculated liquidus projection of the Mn-Ni-Si system in the present work.*

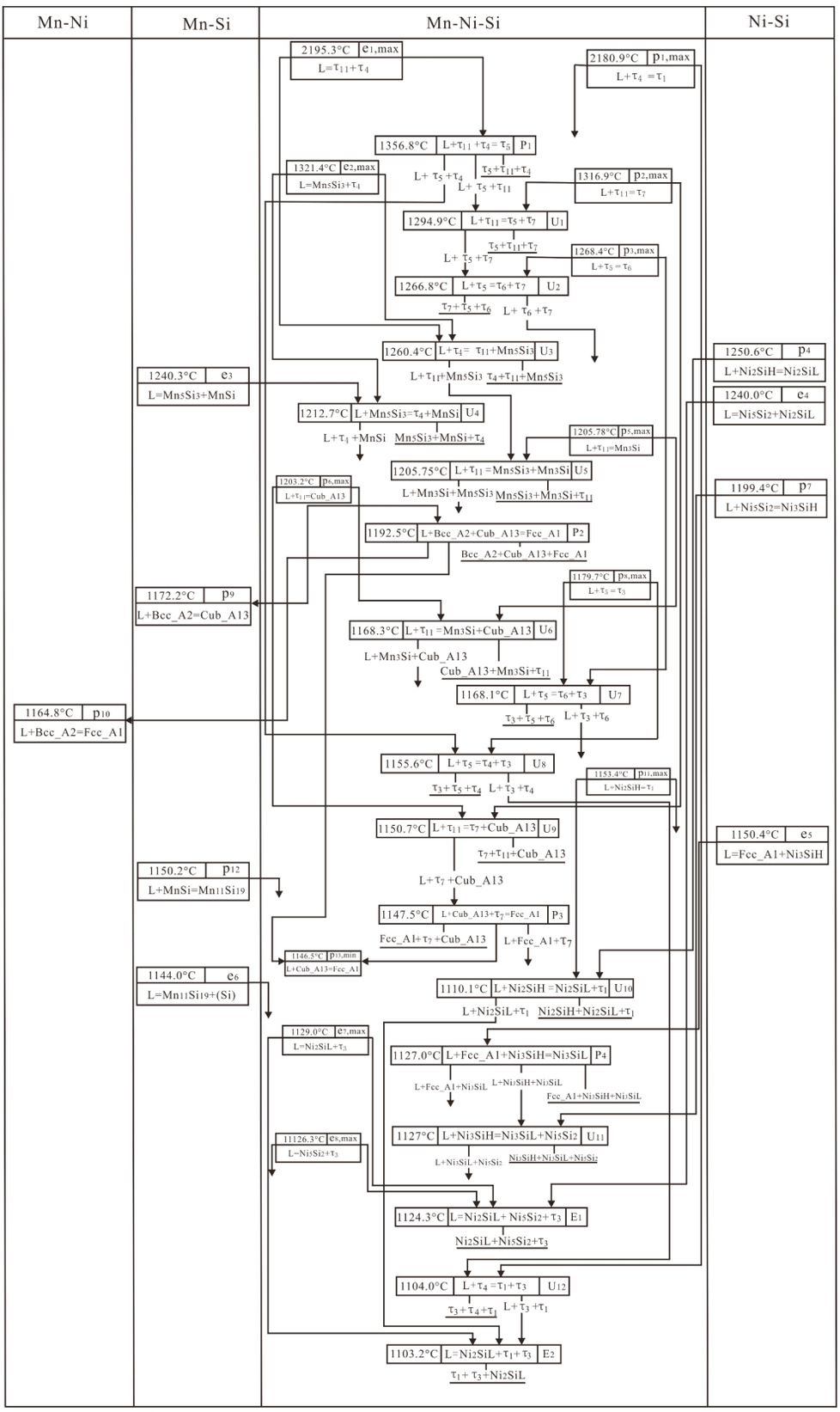

Figure 5. *Reaction scheme for the whole Mn-Ni-Si system according to the present work (part I).*

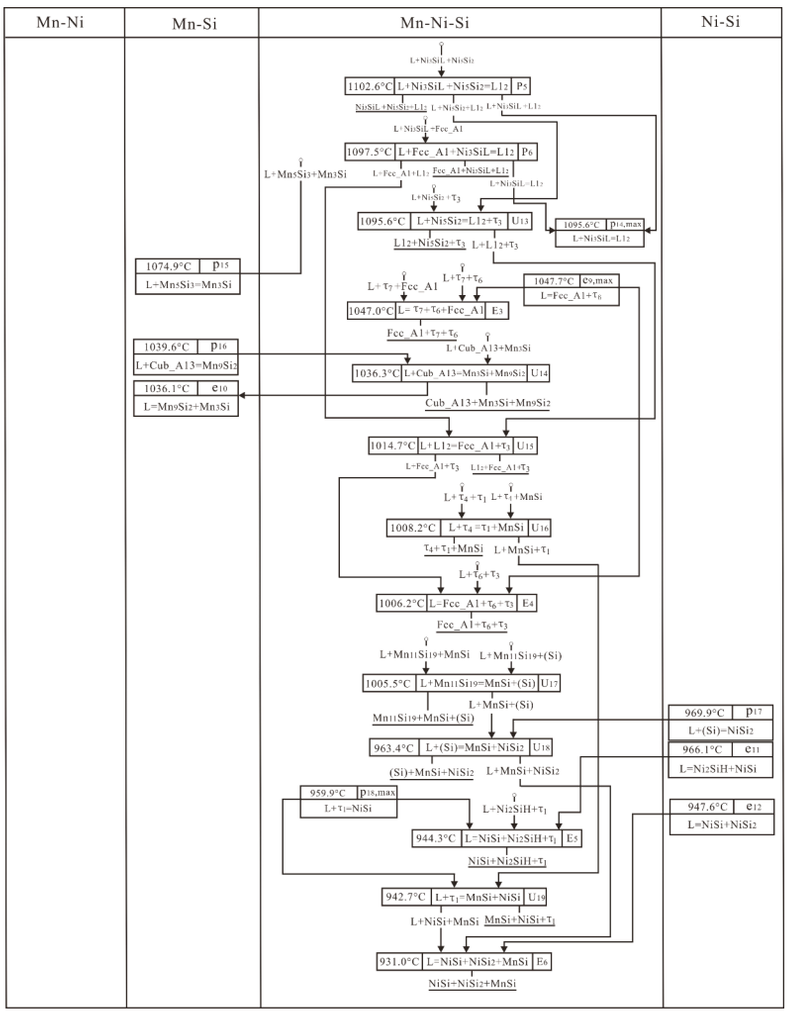

Figure 5. *Reaction scheme for the whole Mn-Ni-Si system according to the present work (part II)*

References

[1] B. Hu, H.H. Xu, S.H. Liu, Y. Du, C.Y. He, C.S. Sha, D.D. Zhao, Y.B. Peng, CALPHAD, 35 (2011) 346-354.

[2] B. Hu, W.-W. Zhang, Y.B. Peng, Y. Du, S.H. Liu, Y.L. Zhang, Thermochim. Acta, 561 (2013) 77-90.

[3] D. Hao, B. Hu, K. Zhang, L.J. Zhang, Y. Du, J. Mater. Sci., 49 (2014) 1157-1169.

[4] Y. Du, S.H. Liu, L.J. Zhang, H.H. Xu, D.D. Zhao, A.J. Wang, L.C. Zhou, CALPHAD, 35 (2011) 427-445.

[5] Z.P. Cao, J.H. Xin, C. Chen, S.H. Liu, B. Hu, C. Tang, Y. Du, J. Min. Metall. Sect. B-Metall., 49 (2013) 307-313.

[6] J. Wang, Y. Du, S.-L. Shang, Z.-K. Liu, Y.-W. Li, J. Min. Metall. Sect. B-Metall., 50 (2014) 37-44.

[7] J.L. Liang, Ph.D. Thesis, Central South University, China, 2011.

[8] Y.Y. Cherkashin, Y.I. Gladyshevskiy, P.I. Kripyakevich, Y.B. Kuz'ma, J. Inorg.Chem. USSR, 3 (1958) 650-653.

[9] Y.B. Kuz'ma, Russ. J. Inorg. Chem., 7 (1962) 691-694.

[10] Y.B. Kuz'ma, E.E. Cherkashin, Dopovidi A. kad. Nauk Ukr, RSR, 10 (1960) 1413-1416.

[11] Y.B. Kuz'ma, E.I. Gladyshevskii, E.E. Cherkashin, Russ. J. Inorg. Chem., 9 (1964) 1028-1031.

[12] D.I. Bardos, R.K. Malik, F.X. Spiegel, P.A. Beck, Trans. Met. Soc. AIME, 236 (1966) 40-48.

[13] K.P. Gupta, J. Phase Equilib., 27 (2006) 529-534.

[14] A.T. Dinsdale, CALPHAD, 15 (1991) 317-425. DOI: 10.1016/0364-5916(91) 90030-N

[15] S.H. Liu, Ph.D. Thesis, Central South University, China, 2010.

[16] Y. Du, Z.P. Jin, B.Y. Huang, W.P. Gong, H.H. Xu, Z.H. Yuan, J.C. Schuster, F. Weitzer, N. Krendelsberger, Metall. Mater. Trans. A, 35 (2004) 1613-1628.

[17] J.C. Schuster, Y. Du, Metall. Mater. Trans. A, 31 (2000) 1795-1803.

[18] O. Redlich, A.T. Kister, Ind. Eng. Chem., 40 (1948) 345-348.

[19] B. Sundman, B. Jansson, J.-O. Andersson, CALPHAD, 9 (1985) 153-190.

[20] Y. Du, R. Schmid-Fetzer, H. Ohtani, Z. Metallkd., 88 (1997) 545-556.